Planck High Frequency Instrument Colour Correction

Locke D. Spencer[A], Giorgio Savini[A,B], Peter A. R. Ade[A], Chris E. North[A], Juan F. Macias-Perez[D], Francois-Xavier Desert[C], and Sergi Hildebrandt[D,E]

[A]School of Physics and Astronomy, Cardiff University, UK.
[B]University College London, London, UK.
[C]Laboratoire d'Astrophysique de Grenoble, Grenoble, France.
[D]Laboratoire de Physique Subatomique et de Cosmologie, Grenoble, France.
[E]California Institute of Technology, Pasadena, California, USA.

Abstract

The spectral response of the HFI detectors [1,2] is determined using ground-based Fourier transform spectrometer (FTS) pre-launch data. These are used to obtain band-average transmission spectra (Fig. 2) and unit conversion/colour correction coefficients. Coefficient maps, based on detector/sky coverage and generated for individual and combined surveys (e.g. S1, S12, S1234, etc.), provide verification of coefficient errors. Maps, histograms, and jackknife tests demonstrate potential biases in data sub-sets.

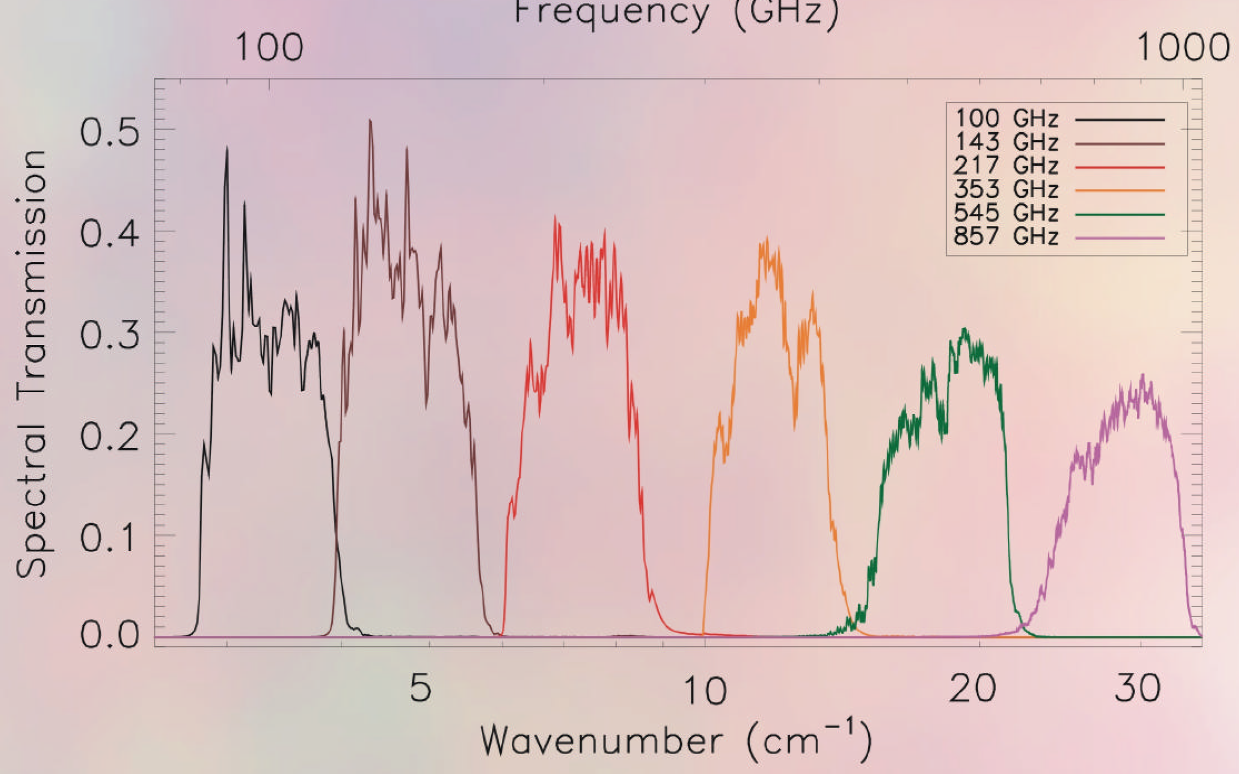

Fig. 1 HFI Band-average transmission spectra.

1. Correction Coefficients

Following the IRAS convention [3], where the product of the flux density and frequency is constant, unit conversion and correction coefficients are derived through equating changes in intensity to convert between K_{CMB}, K_{RJ}, MJy/sr, y_{SZ}, and K_{RJ}km/s CO intensity. Additionally, colour correction coefficients are determined for various spectral indices, β. These relations are as follows

$$U_{\substack{K_{CMB}\\ \text{to}\\ \text{MJy/sr}}} = \frac{\int d\nu\ \tau(\nu) b'_\nu}{\int d\nu\ \tau(\nu)(\nu_c/\nu)} \times 10^{20} \quad \left[\frac{\text{MJy/sr}}{K_{CMB}}\right] \quad , \tag{1}$$

$$U_{\substack{K_{RJ}\\ \text{to}\\ \text{MJy/sr}}} = \frac{\int d\nu\ \tau(\nu) b'_{RJ}}{\int d\nu\ \tau(\nu)(\nu_c/\nu)} \times 10^{20} \quad \left[\frac{\text{MJy/sr}}{K_{RJ}}\right] \quad , \tag{2}$$

$$U_{\substack{K_{RJ}\\ \text{to}\\ K_{CMB}}} = \frac{\int d\nu\ \tau(\nu) b'_{RJ}}{\int d\nu\ \tau(\nu) b'_\nu} \quad \left[\frac{K_{CMB}}{K_{RJ}}\right] \quad , \tag{3}$$

$$U_{\substack{K_{CMB}\\ \text{to}\\ \text{ySZ}}} = \frac{\int d\nu\ \tau(\nu) b'_\nu}{\int d\nu \left\{ \tau(\nu)\,(b'_\nu)\,(T) \left[\left(\frac{h\nu}{kT}\right) \frac{\exp[h\nu/(kT)]+1}{\exp[h\nu/(kT)]-1} - 4 \right]\Big|_{T_{CMB}} \right\}} \quad \left[\frac{y_{SZ}}{K_{CMB}}\right] \quad , \tag{4}$$

$$U_{\substack{K_{RJ}\\ \text{to}\\ \text{ySZ}}} = \frac{\int d\nu\ \tau(\nu) b'_{RJ}}{\int d\nu \left\{ \tau(\nu)\,(b'_\nu)\,(T) \left[\left(\frac{h\nu}{kT}\right) \frac{\exp[h\nu/(kT)]+1}{\exp[h\nu/(kT)]-1} - 4 \right]\Big|_{T_{CMB}} \right\}} \quad \left[\frac{y_{SZ}}{K_{RJ}}\right] \quad , \tag{5}$$

$$U_{\substack{\beta=-1\\ \text{to}\\ \beta}} = \frac{\int d\nu\ \tau(\nu)(\nu/\nu_c)^\beta}{\int d\nu\ \tau(\nu)(\nu_c/\nu)} \quad \left[\frac{\text{Hz}}{\text{Hz}}\right] \quad , \tag{6}$$

and

$$U_{CO} = \frac{\tau(\nu_{CO}) \left(\frac{\nu_{CO}}{c}\right) b'_{RJ}|_{\nu_{CO}}}{\int d\nu\ \tau(\nu) b'_\nu} \quad \left[\frac{K_{CMB}}{K_{RJ}\ \text{km/s}}\right] \quad , \tag{7}$$

where

$$b'_\nu = \frac{\partial B_\nu(T,\nu)}{\partial T}\bigg|_{T=2.725\ \text{K}} = \left[\frac{2h\nu^3}{c^2(\exp[h\nu/(kT)]-1)}\right] \left(\frac{\exp[h\nu/(kT)]}{\exp[h\nu/(kT)]-1}\right) \left(\frac{h\nu}{kT^2}\right)\bigg|_{T=2.725\ \text{K}}, \quad \left[\frac{\text{W}}{\text{m}^2\ \text{sr Hz}\ K_{CMB}}\right] \tag{8}$$

and

$$b'_{RJ} = \frac{\partial B_{\nu\ RJ}(T,\nu)}{\partial T}\bigg|_{RJ} = \frac{2\nu^2 k}{c^2} \quad \left[\frac{\text{W}}{\text{m}^2\ \text{sr Hz}\ K_{RJ}}\right] \quad . \tag{9}$$

Spectral transmission is given by $\tau(\nu)$. The SZ conversion is based on the non-relativistic Kompaneets formula [4]. The CO intensity integral is approximated by a delta function at the CO transition frequency [5].

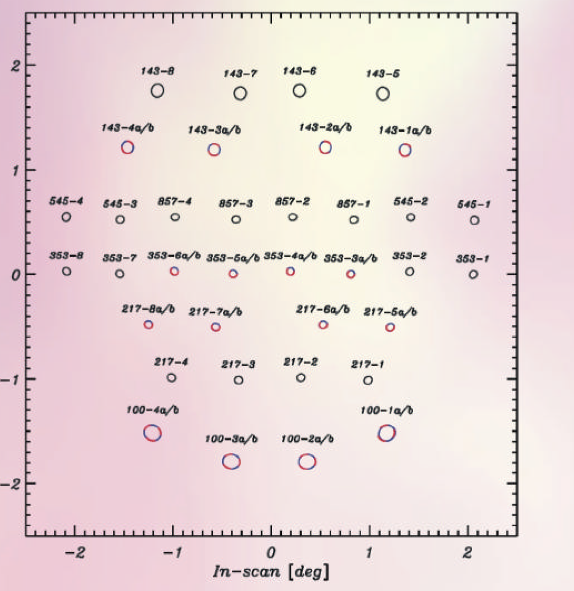

Fig. 2 The HFI Focal Plane on the sky (ellipses-beam FWHM). Fig. from Ref.[1].

2. Band-Average Spectra

Band-average spectra are determined using a noise/CMB weighted average of detector spectra (Eq. 10-12). To incorporate sky coverage into the band-average spectra, detector hit counts, $H_i(\theta,\phi)$, provide integration-time scaled noise estimates, resulting in band-average spectra as a function of sky position, $\tau(\nu,\theta,\phi)$. Coefficient maps are produced through evaluation of Eq. 1-9 for all sky positions, i.e. using $\tau(\nu,\theta,\phi)$ instead of $\tau(\nu)$; yielding Nside=2048 Healpix coefficient maps.

$$w'_i(\theta,\phi) = \frac{H_i(\theta,\phi)/(\text{NET}_i)^2}{\sum_i (H_i(\theta,\phi)/(\text{NET}_i)^2)} \quad . \tag{10}$$

$$w'_{CMB\ i}(\theta,\phi) = \frac{\left[\dfrac{w'_i(\theta,\phi)}{(\Sigma_i w'_i(\theta,\phi))\left(\int d\nu \tau_i(\nu) b'_\nu\right)}\right]}{\max\left\{\sum_i \left[\dfrac{w'_i(\theta,\phi)\tau_i(\nu)}{(\Sigma_i w'_i(\theta,\phi))\left(\int d\nu \tau_i(\nu) b'_\nu\right)}\right]\right\}} \quad . \tag{11}$$

$$\tau_{\text{avg}}(\nu,\theta,\phi) = \sum_i [w'_{CMB\ i}(\theta,\phi)\tau_i(\nu)] \quad . \tag{12}$$

3. Results

The band-average coefficient is positive biased compared to the histogram distribution for the 353 GHz example shown (Fig. 3) and negative biased for the 100GHz case (Fig. 4).

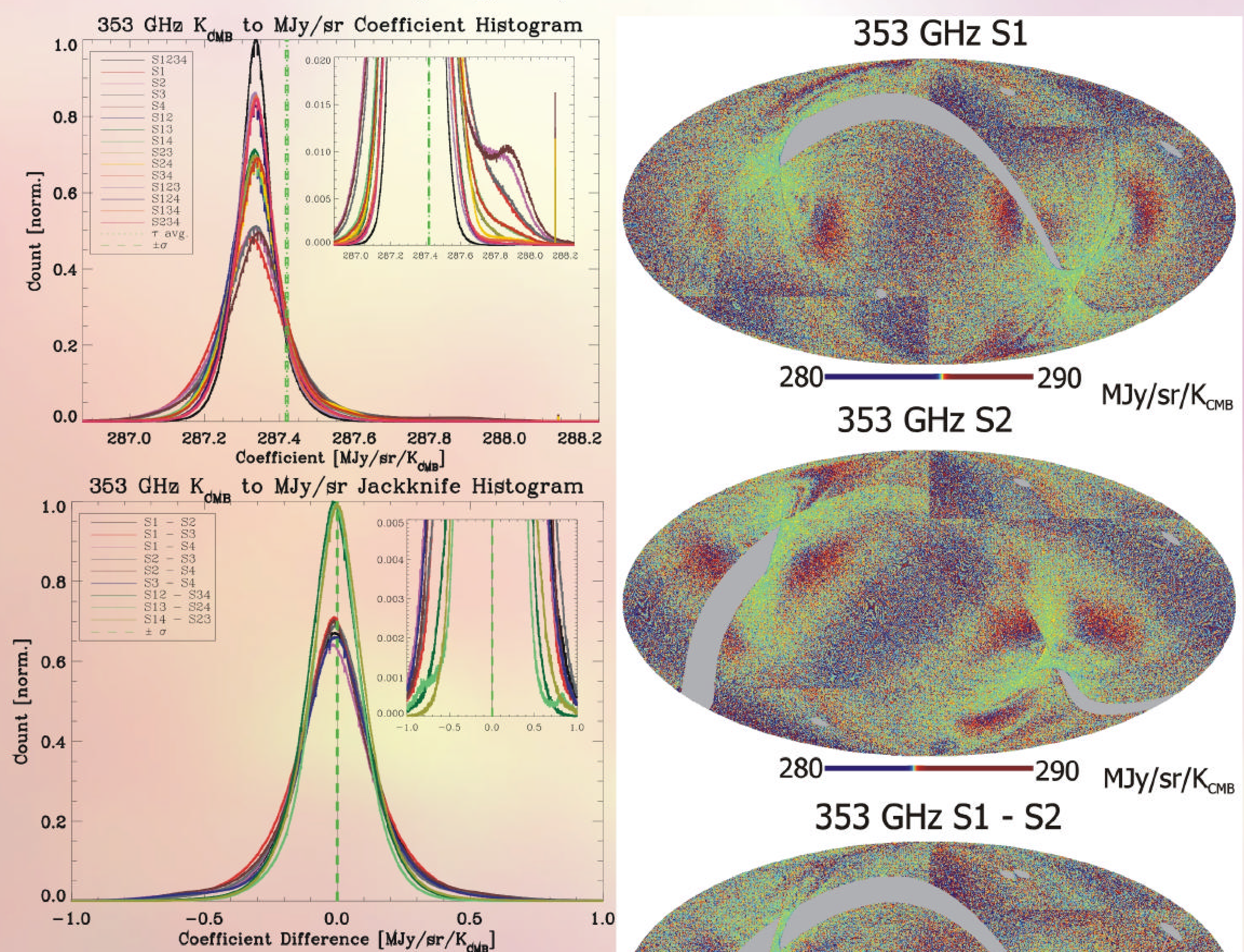

Fig. 3 Histogram (top), and jackknife histogram (centre) of the 353 GHz KCMB to MJy/sr unit conv. coefficient. The right column shows Nside=2048 Healpix maps for S1 (top), S2 (centre), and the S1 - S2 Jackknife map (bottom).

The striping in the maps demonstrates that the histogram outliers are a result of scan strategy. The convergence of coefficients with integration time is shown in the jackknife histograms.

The Cepheus and Perseus regions (Fig. 5), with ancilliary CO data, are used as calibration regions for HFI CO component separation. Uneven scan coverage of the Cepheus region may result in biased correlation of the CO estimate (see stiping in map). The scan coverage of the Perseus region is more uniform.

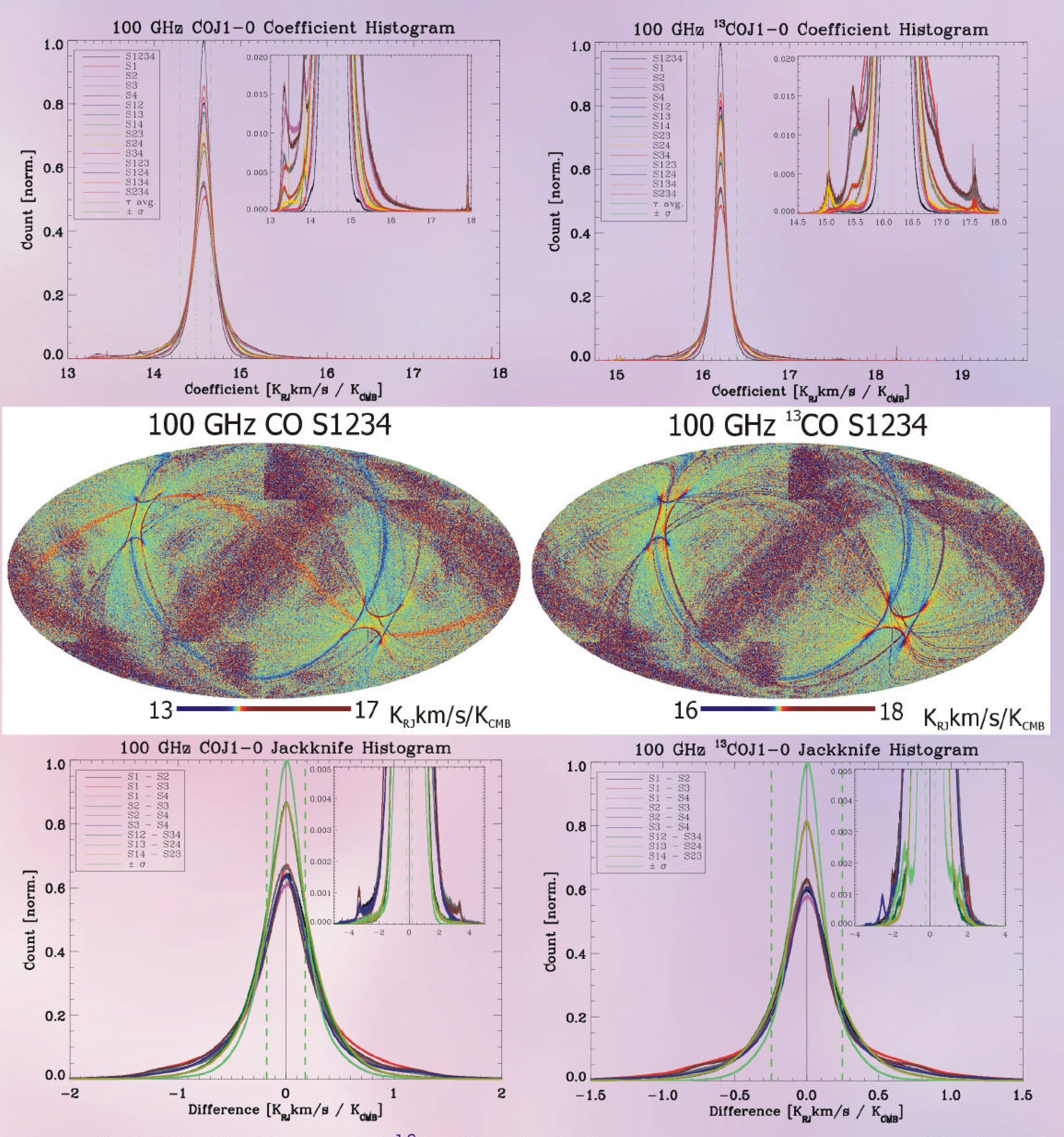

Fig. 4 CO (left) and ^{13}CO (right) conversion coefficient histograms (top), full survey maps (centre), and jackknife histograms (bottom).

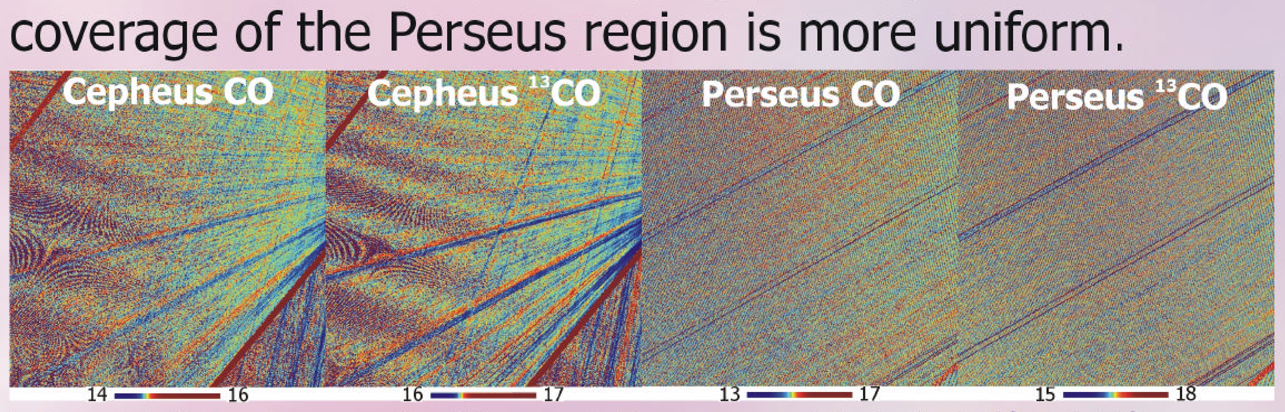

Fig. 5 Cepheus (left) and Perseus (right) 15°x 15° survey 1 coefficient maps for CO (1st of each pair) and ^{13}CO (2nd of each pair).

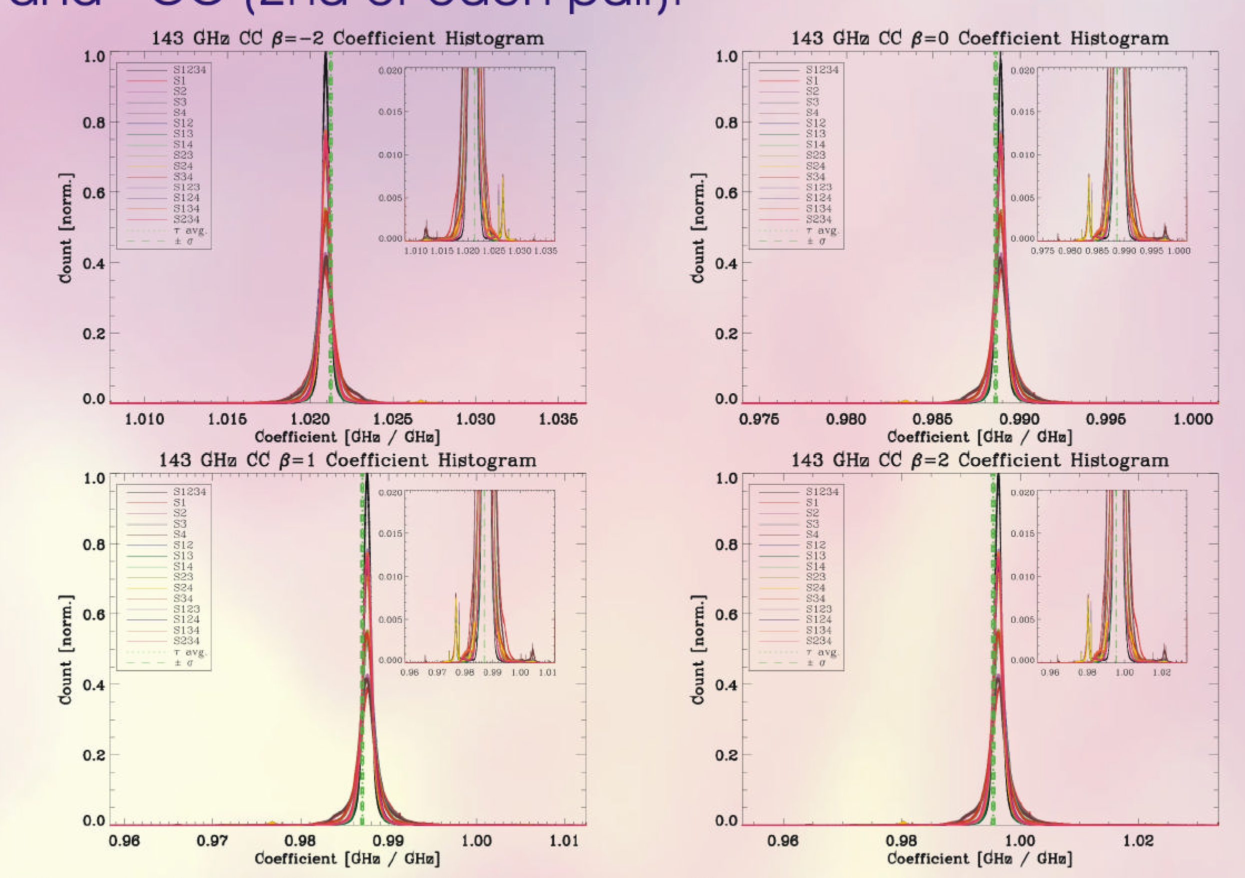

Fig. 6 143 GHz colour correction coefficient histograms for spectral indices of -2 (top-left), 0 (top right), 1 (bottom-left), and 2 (bottom right).

4. Conclusions

This work has shown that sky coverage is an important consideration in the analysis of HFI systematics. The accuracy and bias of band-average correction coefficients has been identified.

References

[1] Planck HFI Core Team, Planck early results. VI. The High Frequency Instrument data processing, A&A 536 A6 (2011), DOI: http://dx.doi.org/10.1051/0004-6361/201116462
[2] Planck HFI Core Team, Planck early results. IV. First assessment of the High Frequency Instrument in-flight performance, A&A 536 A4 (2011), DOI: http://dx.doi.org/10.1051/0004-6361/201116487
[3] California Institute of Technology Infrared Processing and Analysis Center. IRAS Explanatory Supplement, VI. Flux Reconstruction and Calibration, C. Absolute Calibration, C.3 Color Corrections. http://irsa.ipac.caltech.edu/IRASdocs/exp.sup/ch6/C3.html/.
[4] Kompaneets, A. S. 1957, Soviet Phys. JETP, 4, 730
[5] California Institute of Technology Jet Propulsion Laboratory. Molecular spectroscopy catalog, 2004. http://spec.jpl.nasa.gov/.

NSERC CRSNG
Science & Technology Facilities Council
UCL
LAOG Laboratoire d'AstrOphysique de Grenoble
LPSC Grenoble
California Institute of Technology 1891